DOI:10.1021/jf102495s

JOURNAL OF AGRICULTURAL AND FOOD CHEMISTRY
ARTICLE

Lactosomes: Structural and Compositional Classification of Unique Nanometer-Sized Protein Lipid Particles of Human Milk

Nurit Argov-Argaman,*[,†,#] Jennifer T. Smilowitz,[‡,⊗,#] Daniel A. Bricarello,[§] Mariana Barboza,[∥] Larry Lerno,[∥] John W. Froehlich,[∥] Hyeyoung Lee,[‡] Angela M. Zivkovic,[‡,⊗] Danielle G. Lemay,[‡] Samara Freeman,[‡] Carlito B. Lebrilla,[∥] Atul N. Parikh,[§] and J. Bruce German[‡,⊗,⊥]

[†]Department of Animal Science, The Robert H Smith Faculty of Agriculture, Food and Environment, The Hebrew University of Jerusalem, P.O. Box 12, Rehovot 76100, [‡]Department of Food Science and Technology, [⊗]Food for Health Institute, University of California, Davis, California 95616, United States, [§]Department of Applied Science, and [∥]Department of Chemistry, University of California, Davis, California 95616, United States, and [⊥]Nestle Research Center, Lausanne, Switzerland. [#] N.A.-A. and J.T.S. contributed equally to this work.

Milk fat globules (MFGs) are accepted primarily as triacylglycerol delivery systems. The identification of nanometer-sized lipid−protein particles termed "lactosomes" that do not contain triacylglycerol raises the question of their possible functions. MFGs were isolated by slow centrifugation, and lactosomes were isolated by ultracentrifugation at a density equivalent to plasma high-density lipoproteins (HDL) ($d > 1.063$ g/mL) from human milk obtained from six volunteers at different lactation stages. Isolated lactosomes were analyzed and compared with MFGs for their size distribution, lipidome, proteome, and functional activity. Lactosomes from early milk, day 8, were found to be similar in size as those from mature milk >28 days, averaging ∼25 nm in diameter. In total, 97 nonredundant proteins were identified in the MFG and lactosome fractions, 46 of which were unique to the MFG fraction and 29 of which were unique to the lactosome fraction. The proteins identified in the lactosome and MFG fractions were enriched with proteins identified with immunomodulatory pathways. Unlike MFGs and GM1-laden reconstituted HDL that served as a positive control, lactosomal binding capacity to cholera toxin was weak. Lipidomic analyses found that lactosomes were devoid of triacylglycerol and gangliosides, unlike MFGs, but rich in a variety of phospholipid species. The data found differences in structure, composition, and function between lactosomes and MFG, suggesting that these two particles are derived from different biosynthetic and/or secretory pathways. The results reveal a bioactive lipid−protein, nanometer-length scale particle that is secreted into milk not to supply energy to the infant but to play unique, protective, and regulatory roles.

KEYWORDS: Milk; lipidome; proteome; fat globule; lactosome

INTRODUCTION

Throughout evolution, mammalian milk has been subjected to constant Darwinian selective pressure, driving its nutritional values, bioactivities, and complex structures toward an optimization of maternal cost and infant survival (*1*). Synthesis and secretion of complex supramolecular structures into milk are only of value to the extent that they protect the mother and/or encourage the success of the infant. Of all complex structures in milk, our understanding of milk lipid macrostructures is oversimplified, relating primarily to the content of pure triacylglycerols (Tg) and their fatty acid composition. The nutritional properties of milk lipids are treated simply as bulk oils and typically compared to plant-derived oils. However, milk lipids are secreted as ensembles of complex lipid−protein ensembles, termed milk fat globules (MFGs) (*2*).

Unlike other tissues that secrete lipid−protein ensembles in the nanometer length sclae (i.e., lipoproteins), the mammary gland exploits a distinctive synthetic and secretion pathway to deliver lipids throughout an aqueous environment. MFGs are synthesized by the rough endoplasmic reticulum (ER) and exocytosed from the apical side of mammary epithelia enrobed by a trilayer of polar lipids forming the MFG membrane (MFGM) (*3*). The MFGM consists mainly of phospholipids, glycolipids, and sphingomyelin, derived from the ER and the apical membrane of the secreting mammary epithelial cells (*2*, *4*, *5*). These MFGM constituents, both lipids and proteins, have been assigned roles beyond simple nutrition, such as protection against enteropathogens (*6*). The diameters of secreted MFGs range from < 0.2 to > 15 μm (*7*, *8*), and particle size distribution is altered under different physiological and metabolic conditions (*9*−*11*), implying that these disparate particles exert different functions than to simply deliver bulk fat to the infant.

The complexity of the MFG secretion pathway coupled with structural analytical methods ill-equipped to measure structure−function relationships on a nanometer scale, have led to the common perception that MFGs of all sizes share the same synthetic and

*To whom correspondence should be addressed. E-mail: argov@agri.huji.ac.il.

 Published on Web 10/06/2010

secretory pathways. In addition, MFGs of varying sizes are accepted as comparable in composition and function. However, in a recent study, we found that MFGs derived from human milk varied in their lipid composition according to their size (*12*). These results challenged the perception that all MFGs are compositionally identical. Moreover, a class of lipid particles that was not described before was identified on the nanometer scale. These lipid−protein assemblies were termed "lactosomes" to distinguish them from Tg-rich MFGs, a major source of energy for the infant. According to their alleged composition (i.e., lipid−protein, Tg-poor), which is similar to plasma high-density lipoprotein (HDL), lactosomes were isolated in human milk by sequential flotation from the density range corresponding to that of plasma HDL.

In plasma, lipid−protein assemblies within the density of HDL have known functions as transporters of hydrophobic materials form peripheral tissue to the liver (i.e., HDL and albumin). In contrast, the lipid−protein assemblies that play a role in secretion pathway and transport of Tg have lower densities such as low-density lipoprotein and MFG in plasma and milk, respectively. Therefore, the presence of lipid−protein assemblies secreted into milk that are found in milk's high-density range is puzzling and raises questions about their biological roles.

The discovery of this class of lipid particles—lactosomes—in milk that are free of Tg and therefore do not offer a nutritional role to the neonate led us to elucidate their structure and composition to generate new hypotheses with respect to their function.

MATERIALS AND METHODS

Sample Collection and Lipid Particle Separation. Milk samples were collected from six mothers at approximately 10 days, 28 days, and approximately 6 months postpartum. Donors were instructed to fully pump one breast and aliquot 10 mL of milk after gently inverting. Milk samples were stored at −80 °C until further analysis. Samples are denoted by the subject ID, 1000, 1004, 1005, 1006, 1007, and 1008, and postpartum day beginning 24 h after labor, 08, 09, 28, 169, and 198.

Milk lipid particles were separated according to their density. Whole milk was first separated by slow centrifugation at 1000 rpm for 10 min separating skim milk and MFGs as cream. The MFG fraction was gently removed using a wide-opening pipet, to prevent fractionation of the large, Tg-rich milk lipid globules. The skim fraction was respun at 1000 rpm for 10 min to enrich the skim fraction with small particles. This second skim fraction was subsequently adjusted to a density corresponding to that of HDL, 1.063 g/mL (*13*), using KBr solution, and centrifuged for 2 h and 5 min at 120000*g*. The opaque layer formed at the top 300 μL of the vial underneath the fat pad was identified as the lactosome (*12*).

Determining Particle Structure and Sizes. Scanning electron microscopy (SEM) images were obtained of the MFG fraction by washing the fraction in 0.1 M phosphate buffer, pH 7.35, and applying it to poly-L-lysine-treated coverslips (*14*).

Transmission electron microscopy (TEM) was achieved by negative staining the lactosome sample (*15*). A 10 μL drop was added to a 400 mesh form var./carbon grid and incubated for 10 min. Ten microliters of 1% phosphotungstic acid in DDH_2O was added and rapidly blotted from the grid. The particle size for MFG samples was determined by dynamic light scattering using Microtrac S3500 (Microtrac, Montgomeryville, PA) and cited elsewhere (*16*). Particle size data of lactosomes were obtained as described in the Supporting Information text and based on previous lipid vesicles size analysis (*17*).

Identifying MFG and Lactosome Proteome. Lactosomes from samples 1000d08, 1005d08, and 1008d08 were delipidated according to the method of Wessel and Flugge (*18*), and the precipitated protein was solubilized in a solution of 8 M urea, 1% (w/v) SDS, and 100 mM Tris-HCl. Resolubilized protein was then reduced with 200 mM dithiothreitol at 55 °C for 45 min before cooling and alkylation at room temperature with 40 mM iodoacetamide for 20 min in the dark. Reduced, alkylated proteins were then diluted 5-fold with 18 MΩ water and digested overnight with sequencing-grade modified trypsin (Promega, Madison, WI) at 37 °C. The sample was then adjusted to pH 3 with formic acid and desalted on a C_{18} ZipTip.

Analysis was performed using an Agilent 6200 Series HPLC-Chip/TOF MS system equipped with the Agilent 1200 series microwell-plate autosampler, capillary pump, nanopump, and HPLC-Chip interface as described in the SI text. The applied protein identification was achieved by using x! Hunter (version 2009.08.01.3, http://www.thegpm.org/hunter/index.html) to query the Swiss-Prot database (release 15.11). Carbamidomethylation of cysteine residues was selected as a constant modification. Variable modifications included deamidation of asparagine and glutamine residues, oxidation of methionine residues, and acetylation of the N terminus. Semistyle cleavage was not allowed. A single missed tryptic cleavage was allowed for peptide identifications. The species was restricted to *Homo sapiens*.

Analysis of the Lactosome and MFG Proteomes. For each protein in each sample, a percent relative abundance was calculated as (number of total peptides in the sample representing the sequence/number of total peptides identified in the sample) × 100. Using "R" statistical software (http://www.r-project.org/), paired two-sample *t* tests were applied to determine whether each protein's percent relative abundance differed significantly between the lactosome and the MFG fractions. The resulting *P* values are referred to as the unadjusted *P* values, for which $P \leq 0.05$ denotes marginal significance. To improve the stringency of the tests, a Benjamini−Hochberg multiple testing correction was applied to the unadjusted *P* values with functions from the multitest library (*19*). A Benjamini−Hochberg adjusted *P* value ≤0.05 was used to determine significance.

Ingenuity Pathways Analysis software (http://www.ingenuity.com/) was used to identify metabolic and signaling pathways that are over-represented by the MFG or lactosome proteomes relative to all annotated genes. A Fischer's exact test followed by a Benjamini−Hochberg multiple testing correction were used to calculate the *P* value, which represents the probability that the enrichment of the function or pathway with the gene set of interest is explained by chance alone. Functions or pathways reported to be statistically significant were those with a Benjamini−Hochberg adjusted $P \leq 0.05$.

Identification of Particle Function in Binding Cholera Toxin. Spectroscopic analysis of fluorescent probes was performed with an LS 55 fluorescence spectrometer (Perkin-Elmer, Waltham, MA). The primary probe used was 1-(4-trimethylammoniumphenyl)-6-phenyl-1,3,5-hexatriene *p*-toluenesulfonate (TMA-DPH) from Invitrogen (Carlsbad, CA), which only fluoresces from within a hydrophobic environment. After a 30 min delay to allow DPH partitioning into the lipid portion of the sample, cholera toxin subunit B (CTB, Sigma-Aldrich, St. Louis, MO) modified with a fluorescent tag (fluorescein isothiocyanate or FITC) was added. As FITC-CTB associates with GM1 at the particle surface, the close proximity of the FITC dye molecule to the DPH contained in the lipid bilayer of the particle induces nonradiative energy transfer from donor (DPH) to acceptor (FITC); also known as FRET or Forester resonance energy transfer. The association of CTB with milk particles can thus be identified by measuring the reduction in DPH emission and a qualitative comparison generated between samples and controls. Fluorescence emission was monitored using a fluorescence spectrometer at a wavelength of 490 nm, which corresponds to peak FITC absorption (*20*). Donor−acceptor (i.e., TMA-DPH and FITC-CTB) concentration ratios were kept constant across all samples. In addition, a similar lipid to probe ratio was maintained in each sample to minimize systematic variation in donor−acceptor spacing and to ensure a qualitative comparison remains valid. All scans were performed at a temperature of 37 °C and pH 7.4. Reconstituted HDL (rHDL) were produced as previously described (*21*) using purified wild-type apolipoprotein AI (apoAI) that was a gift from Dr. John C. Voss's lab.

Identifying the Lipidome of MFG and Lactosome Fractions. MFG fraction lipids ($n = 3$) were extracted by the Folch method with the final lipid extract dissolved in 1 mL of $CHCl_3$ and stored at −80 °C until analyzed (*22*). A modified Folch extraction was used to extract lipids from lactosome samples that matched the MFG fractions analyzed ($n = 3$) as described in the Supporting Information.

Mass Spectrometric Comparison of Lipid Extracts. The MFG fraction lipid extracts were prepared for analysis by mass spectrometry by diluting the sample 500-fold using a solution of CH_3Cl:MeOH (1:2 v/v) spiked with 10 mM NH_4Ac. Lactosome lipid extracts were prepared for mass spectrometric analysis by performing a 5-fold dilution using the same solution as that used for the MFG fraction extracts. MFG fraction samples were analyzed in the positive mode, whereas the lactosome samples were analyzed in both the positive and the negative mode using electrospray

ionization on a Varian 920 TQ-FTMS Fourier transform ion cyclotron resonance mass spectrometer (ESI FT-ICR MS) (Varian Inc., Walnut Creek, CA) equipped with a 9.4T superconducting magnet (Cryomagnetics, Oak Ridge, TN) and as described in the Supporting Information.

Determining the Presence of Gangliosides in MFG and Lactosome Fractions. Gangliosides were extracted from desalted MFG and lactosome fractions as previously described with several modifications (*23*, *24*). Briefly, samples were mixed with 22.5 volumes of water/chloroform/methanol 1.2:1:2 (by volume) and centrifuged at 2000 rpm, and the aqueous upper layer was collected. The pellet was re-extracted with water/chloroform/methanol 1.2:1:2 (by volume) and centrifuged, and the aqueous layer was combined. The gangliosides were then enriched and purified by DEAE-Sephadex anion exchange column (GE Health Care Bio-Sciences, Little Chalfont, United Kingdom) and C8 solid phase extraction (Supelco, Bellefonte, PA). The dried samples were solubilized in a 50:50 (v/v) methanol/water solution prior to mass spectrometry analysis.

Mass spectra were acquired on an IonSpec Pro MALDI FT-ICR mass spectrometer with a 7.0 T superconducting magnet (IonSpec, Irvine, CA) in positive and negative ion modes. Microliter quantities of an analyte solution and a matrix solution were mixed on a sample plate. A 50 mg/mL 2,5-dihydroxybenzoic acid amount in a 50:50 acetonitrile/water was used as the matrix. A standard ganglioside mixture was used for external calibration.

RESULTS

Characterization of Human MFG and Lactosome Fractions. The morphology of MFGs in cream isolated from mature milk was analyzed by SEM, and lactosome particles isolated from the same milk samples were analyzed by TEM. The size distribution of MFGs was within the size range of previously reported data (**Figure 1A**) (*16*). Unlike MFGs, the size distribution of lactosomes was strikingly homogeneous and an order of magnitude smaller (~25 nm) (**Figure 1B**).

Dynamic light scattering was used to confirm the size ranges for both MFGs and lactosome particles from the same milk samples. Mean diameters of MFGs in the cream fractions were 2.7 ± 0.9, 1.5 ± 0.7, and 1.3 ± 0.6 μm, from samples 1000d9, 1004d8, and 1005d8 respectively. Dynamic light scattering confirmed the size and homogeneity of lactosomes visualized by TEM (**Table 1**) using a 90Plus Particle Size Analyzer (Brookhaven, Holtsville, NY). Interquartile ranges for lactosome size distributions were generated from repeated particle dynamic size measurements for each sample (**Figure 2**) and indicated a narrow size distribution. Because of unequal numbers of size values generated among early and mature lactosomes, an independent samples *t* test that assumed heteroscedasticity found significant differences between early and mature lactosomes for sample 1004 ($P \leq 0.05$); however, there were no significant differences between lactation stages for samples 1000 and 1005.

Proteomes of MFG and Lactosome Fractions Differ in Composition and Share Functions in Immunomodulation. In addition to characterizing the morphologic structure of lactosomes, proteomic analyses of three lactosome samples and paired MFG fractions were determined by LC-MS-MS. The proteins identified in the lactosome and MFG fractions included caseins, abundant whey proteins (including α-lactalbumin, lactoferrin, osteopontin, and bile salt-stimulated lipase), and several known MFG proteins (butyrophilin and various apolipoproteins). In total, 97 nonredundant proteins were identified in the MFG and lactosome fractions, 46 of which were unique to the MFG fraction and 29 of which were unique to the lactosome fraction (Supporting Information, Tables 1−6).

To elucidate functions of MFGs and lactosomes, their proteomes were analyzed for the enrichment of functions and signaling pathways. Significant molecular and cellular functions associated with the lactosome fraction are listed in **Table 2** in order of decreasing significance. With the exception of "amino acid metabolism", MFGs shared these functions. In addition, the MFG proteome was associated with "cell signaling" and "free radical scavenging". Two signaling pathways were enriched with proteins identified in the lactosome: "acute phase response signaling" and "caveolar-mediated endocytosis signaling". Both of these pathways, as well as a number of other immunomodulatory pathways, were enriched with proteins identified in MFGs. Both MFG and lactosome proteins clearly have many possible immunomodulatory functions, suggesting that lactosomes, like MFG, are important to the protection of the neonate.

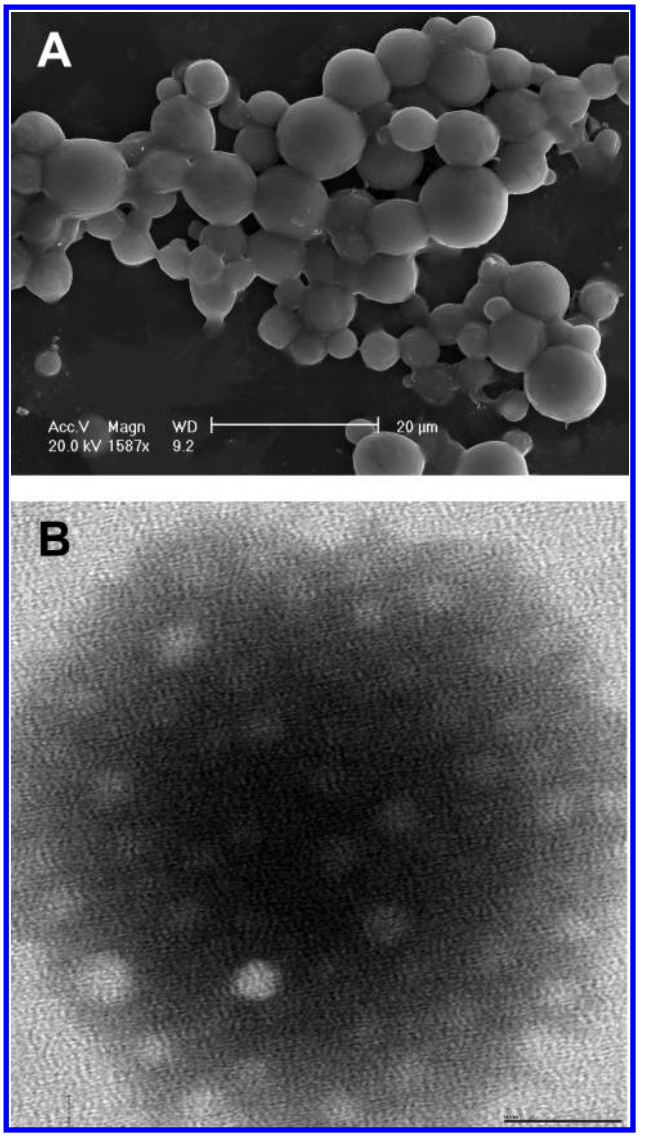

Figure 1. Images of milk fat globules (MFG) and lactosome fractions. (**A**) SEM of the MFG fraction at 169 days postpartum (bar = 20 μm). (**B**) TEM of the lactosome fraction at 169 days postpartum (bar = 50 nm).

Table 1. Size Characteristics of Lactosomes[a]

	nm		
sample	mean	median	range
1000d09	30.5 ± 14.7	28.5	8.6−81.1
1000d28	26.1 ± 13.1	23.8	5.2−54.8
1004d08	34.2 ± 16.4	33.1	10.0−74.5
1004d28	24.2 ± 12.0*	22.2	8.8−69.0
1005d08	24.5 ± 13.6	19.9	9.4−61.3
1005d28	28.3 ± 16.4	22.8	8.5−67.0

[a] Data displayed as means ± standard deviations; different from day 08, $P < 0.001$.

To determine whether relative abundances of proteins differ between the MFG and the lactosome fractions, paired two-sample *t* tests were applied to abundances of the 97 nonredundant proteins in the MFG and lactosome samples. Of the 97 proteins, 21 were marginally significant (unadjusted $P \leq 0.05$), two of which, immunoglobulin heavy constant α 1 (IGHA1) and carbonic anhydrase 6 (CA6), were significant after a multiple testing correction (B−H adjusted $P \leq 0.05$). The percent abundances of these 21 proteins in the two fractions are depicted in **Figure 3**.

MFG and Lactosome Fractions Differ in Lipid Composition. To further our understanding about the functional roles of human milk particles, preliminary lipidomic analyses were generated and compared between MFGs in cream and lactosomes from the same three subjects during the same lactation stage. On the basis of the reported literature concerning the lipid composition of human milk fat, the decision was made to collect positive mode spectra of the MFG fraction as this fraction was expected to be composed largely of Tg (*25*, *26*), which are best detected in the positive mode. The positive mode mass spectra of the lipids in the MFG fraction showed several clusters of protonated masses

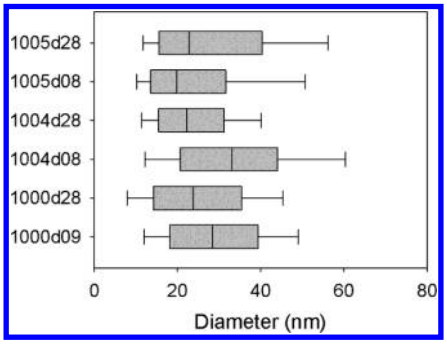

Figure 2. Size distribution of lactosomes derived from early and mature milks from various donors. Each box plot represents the distribution of repeated particle diameter measurement using a commercial dynamic light scattering device. The first four digits denote the sample donor (1000, 1004, and 1005), while the final two indicate the postpartum day after labor (08, 09, or 28).

separated by 28 mass units with each cluster being composed of several distinct masses in the *m*/*z* 700−900 range. These clusters can be seen in **Figure 4A**, an ESI FT-ICR spectrum of the MFG fraction from sample 1008 day 8. It was determined that each of these clusters was a family of lipids differing only in the degree of saturation. The high resolving power and mass accuracy afforded by FT-ICR MS allowed these lipids to be identified as glycerides, specifically Tg. While the class of the lipids in the spectra could be assigned on the basis of accurate mass measurements, the constituent fatty acids, and their position within the lipid, could not be conclusively identified. Further analysis of the lipids by tandem mass spectrometry will be required to obtain these results. Dimers of fatty acids were also seen in the positive mode spectra of the MFG fractions in the range of *m*/*z* 500−600 (**Figure 4A**, marked with triangles). The formation of lipid dimers, trimers, and higher aggregates during the electrospray process is well-known and not unexpected when the total lipid content of the electrospray solution is greater than 0.1 ng/mL (*27*). Tandem mass spectrometry experiments confirmed these ions as being dimers of long chain fatty acids (Supporting Information, Figure 1). It should be noted that although monoacylglycerol, diacylglycerol, phospholipids, and glycolipids were not identified in these spectra, they are most likely in the MFG fraction but cannot be detected due to limited dynamic range of FT-ICR MS. The negative mode spectra of the MFG fraction showed few detectable lipid masses, with the few detected lipids being the deprotonated analogues of the fatty acid clusters in the positive mode spectra. Because the lipidome of human milk is known (*28*), it was decided to proceed with MFG analysis in positive mode only since MFG are predominately Tg.

The positive mode spectra of the lactosomes showed possible ammoniated phosphatidylcholine, phosphatidic acid, and cholesterol ester species in very low abundance (< 1% of the spectral intensity) in the range of *m*/*z* 700−900, while the dominant species in the spectra were nonlipid (Supporting Information, Figure 2). Comparison of the positive mode spectra for the MFG and lactosome fractions clearly shows that the two have different lipid compositions. Because of the extremely low abundance of the potential lipid ions, further study is needed to determine an

Table 2. Significant Molecular and Cellular Functions Associated with the Lactosome Fraction

significant function	associated proteins
lipid metabolism	APOE, APOB, APOA1, CLU, BTN1A1, LALBA, CEL, ALB, LTF, PLIN2, PSAP, SERPINA1, FABP3
molecular transport	B2M, APOE, TTR, APOB, APOA1, CLU, BTN1A1, LALBA, CEL, ALB, LTF, PLIN2, CSN2, PSAP, FABP3
small molecule biochemistry	APOE, GNPDA1, TTR, APOB, APOA1, CLU, LALBA, BTN1A1, LYZ, CEL, ALB, LTF, PLIN2, PSAP, SERPINA1, FABP3, KRT1
protein synthesis	APOE, APOB, APOA1, CSN2, LALBA
cellular movement	APOE, CD59, SPP1, APOB, CFL1, APOA1, CLU, LIMS1, KRT10, PIGR, ACTG1, ALB, SERPINA1, C4B
cellular assembly and organization	B2M, APOE, CD59, TTR, SPP1, CFL1, APOA1, SEPT7, CLU, MFGE8, KRT9, CST3, PLIN2
cell death	PKM2, B2M, APOE, TTR, CD59, APOB, SPP1, CFL1, APOA1, CLU, YWHAZ, LIMS1, LALBA, MFGE8, LYZ, KRT10, PIGR, ALB, CST3, PSAP
carbohydrate metabolism	PKM2, CEL, APOE, ALB, GNPDA1, SPP1, APOA1, PSAP, LALBA, LYZ, FABP3
amino acid metabolism	APOE, TTR, ALB
cell-to-cell signaling and interaction	B2M, APOE, TTR, CD59, SPP1, APOB, CFL1, APOA1, CLU, MFGE8, LIMS1, LYZ, PIGR, ALB, LTF, KRT2, KRT1, C4B
antigen presentation	APOE, APOB, SPP1, APOA1, KRT1, PIGR, C4B
cellular growth and proliferation	B2M, APOE, CD59, SPP1, CFL1, TFG, APOA1, CLU, MFGE8, KRT10, MYOF, PIGR, CST3, KRT2, SERPINA1, FABP3, KRT4
protein trafficking	APOE, APOA1, CSN2, LALBA
gene expression	PIP, SPP1, CLU, YWHAZ, LALBA
cellular compromise	APOE, SPP1, CFL1, SEPT7, CLU
cell morphology	B2M, APOE, SPP1, LTF, CFL1
cellular development	B2M, APOE, CD59, SPP1, CST3, CLU
cellular function and maintenance	KRT9, APOE, CD59, SPP1, CFL1, CST3, CLU
post-translational modification	CEL, APOE, ALB, C4B
vitamin and mineral metabolism	APOE, CEL, APOA1, PLIN2, KRT1

enrichment procedure to elucidate their structure and determine if they are truly cholesterol esters.

The predominant lipid species in the negative mode spectra of the lactosome fractions were identified as inositol species and phosphatidic acids (**Figure 4B**, marked with a star). Fatty acid dimers were also seen in the negative mode spectra but at much less abundance than in the MFG fractions. On the basis of these preliminary results, it can be seen that the MFG and lactosome fractions are clearly different with regards to lipid composition. A more in-depth lipidomic analysis as well as the development of methods to enrich the lactosome lipid extracts will be the topic of future work.

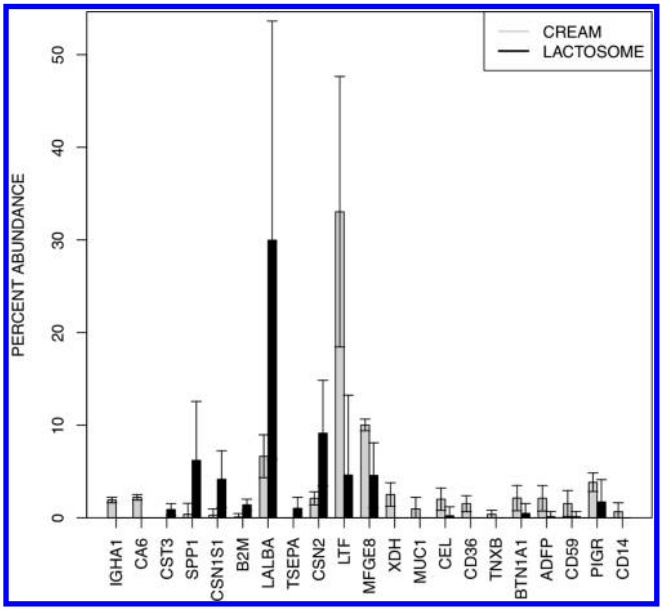

Figure 3. Differences in protein abundance between MFGs and lactosome fractions. The relative abundances of proteins differ between the MFG and the lactosome fractions (marginal significance, unadjusted $P \leq 0.05$). Two of these proteins, immunoglobulin heavy constant α 1 (IGHA1) and carbonic anhydrase 6 (CA6), were significant after a multiple testing correction (B−H adjusted $P \leq 0.05$).

The mass spectrum of the purified MFG gangliosides shows individual ganglioside species and high heterogeneities in ceramide structures (**Figure 5**). Each peak was tentatively assigned based on accurate mass measurements with the postulation of core structures. For example, the $[M - H]^-$ ion at m/z 1235.799 and the $[M + Na - 2H]^-$ ion at m/z 1548.877 corresponded to Neu5Ac-Gal-Glc-Cer (d40:1) and Neu5Ac-Neu5Ac-Gal-Glc-Cer (d40:1), respectively. Sequences of the gangliosides reported herein are consistent with those of the previously reported human milk ganglioside GM3 and GD3 (*29*). However, following the same procedure, only noise peaks were observed, and gangliosides were not detectable from lactosomes (Supporting Information, Figure 3).

MFGs in Cream Offer Protection against Cholera Toxin Binding. To directly probe whether human MFGs or lactosomes impart protective biological functions, a FRET-based assay was performed to assess cholera toxin-receptor binding. Positive controls of vesicles and rHDL (**Figure 6A**) synthesized with DMPC and the cholera toxin receptor, GM1 showed binding while negative controls of vesicles and rHDL without GM1 displayed little or no measurable binding. The addition of CTB to the MFG fraction derived from human milk led to a significant decrease in fluorescence indicating binding. However, after addition of CTB to paired lactosomes, the magnitude in fluorescence was comparable to that of the negative controls (**Figure 6B**). These data indicate that MFGs, known to contain gangliosides (*25*), bind pathogenic toxins (*30*, *31*) and hence are capable of intercepting pathogenic toxins specific to cholera. Lactosomes, although rich in phospholipids, do not contain appreciable concentrations of gangliosides and may provide biological protection through immunomodulation rather than as a vector to thwart pathogen or toxin binding.

DISCUSSION

In this study, an interdisciplinary approach was applied to compare the structure, composition, and putative functions of unique lipidated nanometer-length particles, in human milk, recently termed

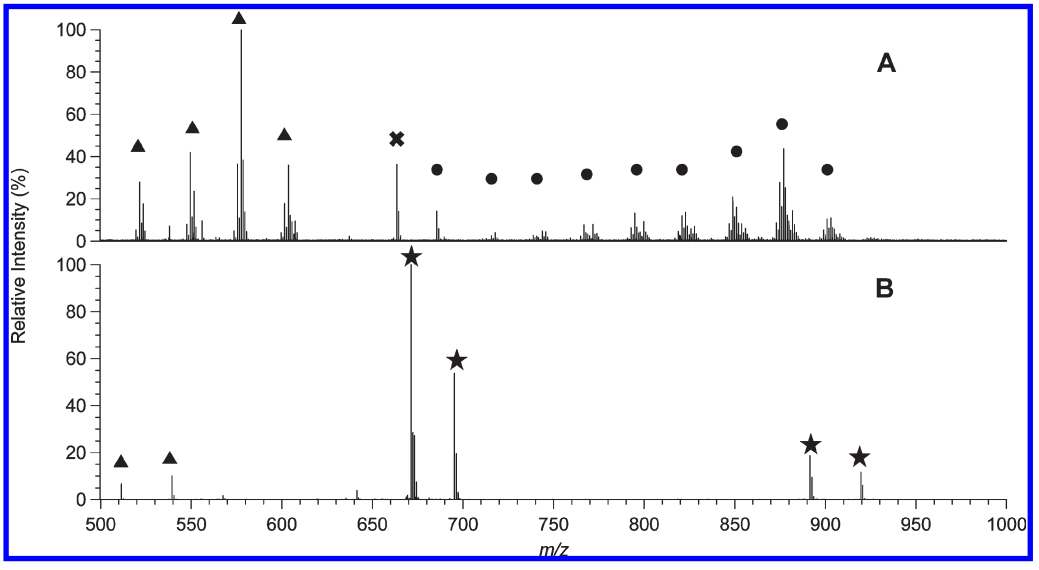

Figure 4. ESI FT-ICR MS spectra of MFG and lactosome fractions from sample 1008 day 8 showing marked distinctions. (**A**) Positive mode spectrum of the MFG fraction. The MFG spectra are dominated by triglyceride (Tg, marked with a circle) and dimers of long chain fatty acids (marked with a triangle). Lipid heterogeneity can clearly be seen in the Tg species. (**B**) Negative mode spectrum of the lactosome fraction showing phospholipid (Pl, marked with a star) and fatty acid dimers (marked with a triangle). The phospholipids identified in this spectrum were phosphatidylinositol (m/z 890−920), bisphosphotidylinositol (m/z 670−700), and phosphatidic acid (m/z 640−650).

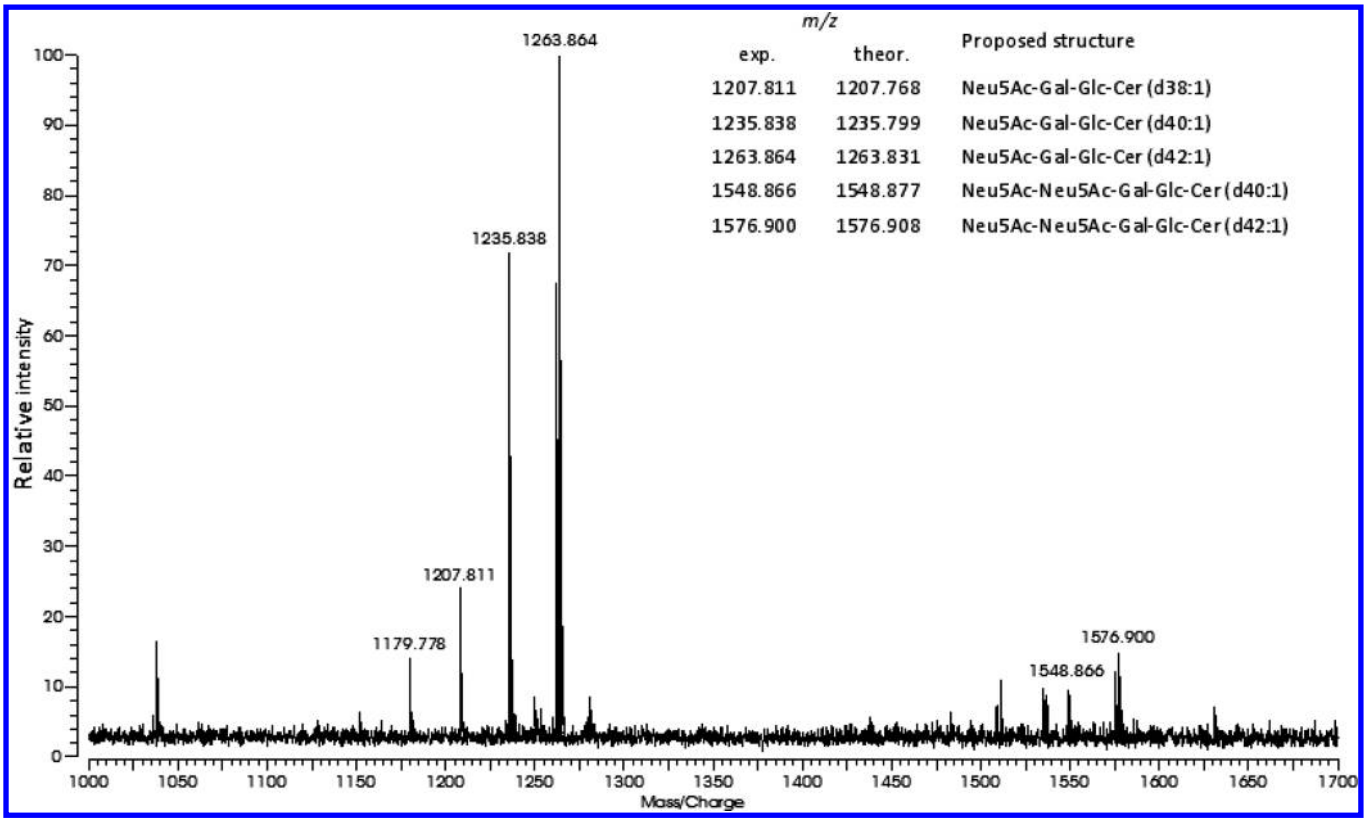

Figure 5. Negative mode spectrum of human MFG gangliosides for 1005d28. The legend in the figure lists the assignment of the major detected structures shown.

lactosomes (*12*). Proteomic shotgun analysis combined with lipidomics and fluorescence-based techniques yielded the initial functional characterization of human lactosomes.

Using TEM, isolated lactosomes from milk collected at 10 days postpartum were visualized as spherical particles of approximately 25 nm in diameter. To acquire a more accurate size distribution of the lactosomes from varying lactation stages (days 8, 9, and 28) from three subjects, dynamic light scattering was used. Lactosomes isolated from early and later lactation stages were about 30 nm in diameter, which is similar to that of stable vesicles, yet, dissimilar in size to plasma HDL (*32*). Similarly, lactosomes diameter and size distribution were much smaller than other milk-derived nanovesicles of unknown origin—exosomes (*33*).

Lactosomes are spherical lipid particles in milk, and it was initially suspected that they were compositionally and functionally similar to MFGs. Because the MFG size distribution is sufficiently wide such that the smallest MFG can overlap with the largest lactosome particles, size alone cannot determine if lactosomes are small MFGs. Therefore, a shotgun proteomic analysis was conducted to compare functional differences between lactosome and MFGs from paired samples. In a first pass annotation approach, ingenuity pathways analysis was used to connect the complex array of proteins that were identified in the lipid particles to biological processes. Admittedly, this approach is limited since most genes and the proteins that they encode have not been annotated for cellular functions and not milk and lactation-related functions. Nevertheless, the plethora of molecular functions represented by proteins in the lactosome fraction coupled with the absence of triglyceride content suggests that lactosomes may provide a unique delivery mechanism for transfer of signaling proteins between mother and offspring.

To interrogate the possibility that lactosomes do not share an identical secretion pathway with Tg-rich MFGs, a manual screening of proteins with differing abundance between MFGs and lactosomes (**Figure 3**) was conducted using the amiGO Web site (http://amigo.geneontology.org/cgi-bin/amigo/search.cgi). The proteomic results confirm that several membrane-bound proteins that are well-described as part of the apical membrane of the mammary gland epithelial cell were only found in the MFGs and not in the lactosomes. MUC1 (mucin 1), which was significantly associated with the MFGs and not the lactosomes, is found on the apical membrane of mammary epithelial cells. Its presence in the MFGs is in agreement with the known and unique secretion pathway in which globules bud from mammary epithelium enveloped by the apical membrane of the cells, including its cargo of proteins. The absence of MUC1 from the lactosomes proteome further distinguishes it from milk exosomes, which were reported to carry a substantial amount of this glycoprotein on their surface (*33*). Similarly, IGHA1 is also associated with the MFG and not the lactosomes. IGHA1 is associated with the ER—the site of Tg synthesis—of the mammary epithelial cell. On the other hand, MFGE8 (MFG-EGF factor 8 protein), a protein that interacts specifically and noncovalently with phosphatidylserine and phosphatidylethanolamine, was found in both MFGs and lactosomes. The presence of this protein in both MFGs and lactosomes confirms that phospholipids surround both particles. Finally, two well-defined proteins, XDH (xanthine dehydrogenase) and BTN1A1 (butyrophilin), known for their major role in the secretion pathway of Tg-rich MFGs (*34*), were unequally associated with each of the studied particles. XDH was found only in the MFG, whereas BTN1A1 was found in both MFGs and lactosomes, however, in much lower abundance in the latter. These two proteins and the interaction between them are required for the secretion of Tg-rich MFGs, and their absence or low abundance in lactosomes suggest that lactosomes are secreted by a different pathway.

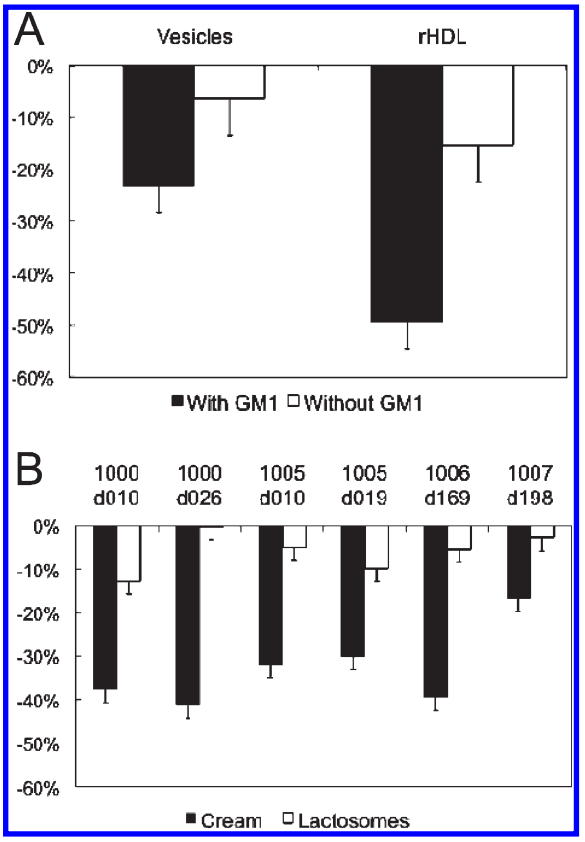

Figure 6. Cholera toxin binding assay. (**A**) Positive and negative controls for the cholera toxin binding assay. Dimyristoylphosphatidylcholine (DMPC) vesicles and rHDL (containing DMPC and apolipoprotein A−I) were prepared for comparative analyses with the MFG and lactosome fractions. Positive controls were laden with 1 mol % GM1 (toxin receptor), while negative controls did not contain any GM1. The graph shows the percent drop in DPH fluorescence at 490 nm for each control sample. (**B**) Cholera toxin binding in response to MFG and lactosomes. The percent drop in donor emission (DPH) after introduction of FITC-labeled cholera toxin is shown here. The lactosome fractions do not show a significant reduction relative to the negative controls, while the MFG fractions are comparable to the positive controls.

The annotated functions of those proteins with greater abundance (unadjusted $P \leq 0.05$) in the lactosomes relative to the MFGs suggest that lactosomes have putative protective roles in immunity and cell regulation. SPP1 (osteopontin), an extracellular glycoprotein associated with the aqueous phase of colostrum (*35*) involved in the early innate (*36*) and adaptive immune responses (*37*−*39*). Another lactosome-associated protein found in the aqueous phase of human colostrum (*35*) with immune-modulatory function is B2M (β-2-microglobulin). B2M is a component of the major histocompatibility complex (MHC) class 1, associated with the acute phase response (*40*) and shown to be critical for protection against bacterial infection. In addition to carrying a protein cargo associated with immune protection, lactosomes offer a putative role in protection against dysregulated cellular proliferation. Lactosomes contained a relatively high abundance (unadjusted $P \leq 0.05$) of LALBA (α-lactalbumin), a major secretory protein of human whey (*35*) and a component to lactose synthase. In the presence of oleic acid, partial unfolding of α-lactalbumin is engineered into HAMLET (human α-lactalbumin made lethal to tumor cells), which acts as an apoptotic factor that has the ability to kill abnormal cells, while sparing healthy ones (*41*, *42*). Thus, it is possible that lactosomes have a distinct function in the protection of the neonate gut.

To confirm that the lipid components of MFGs and lactosomes are compositionally different, mass spectrometry analysis was performed. The analysis of the mass spectra obtained from MFGs and lactosome samples found fundamental differences between the two fractions. The MFG predominantly contained triacyl and diacylglycerol, which were absent in lactosomes. The predominant lipid classes found in lactosomes were phospholipids. On the basis of the absence of a Tg core, an energy delivery role cannot be assigned to lactosomes unlike that for MFGs.

To elucidate the functional role associated with both MFGs and lactosome particles, both were tested in a positive- and negative-controlled cholera binding functional assay. Lipid−protein assemblies from plasma (i.e., lipoproteins) (*43*, *44*) and from milk (*45*) exert protection against endotoxemia by binding and neutralizing bacterial-secreting toxins. In spite of their low abundance in milk as part of the MFGM, gangliosides play an important role in the prevention of infection and immunity (*31*, *46*). Therefore, we tested if milk-derived lipid−protein assemblies could bind cholera toxin as compared with rHDL and MFGs. Because GM1 binds endotoxins with a high affinity (*47*), the positive and negative controls for this assay included rHDL and phospholipid vesicles laden with and without ganglioside monosialyic (GM1). Interestingly, while Tg-rich MFGs showed significant binding capacity as compared with the positive controls, the lactosomes showed little interaction with cholera toxin. Not knowing if this was a result of the compositional or structural configuration of lactosomes, gangliosides were measured and compared between lactosomes and MFGs.

Gangliosides were not detected in the lactosomes; however, GM3 and GD3 were identified in MFGs. These data together with the proteomic analyses do not support the current accepted theory in which all milk-derived lipid particles originate from the same synthetic and secretory pathways in the mammary gland (*2*). Furthermore, the difference in ganglioside composition—a signature of the apical mammary epithelial cell membrane—suggests that lactosomes do not share the secretory pathway with MFGs.

Our data indicate that milk contains at least two different species of lipid−protein assemblies, MFGs and lactosomes. On the basis of their different lipid and protein compositions, MFGs and lactosomes appear to be secreted from different synthetic and secretory pathways. Using shotgun proteomic analysis, both particles were found to carry a cargo of proteins involved in inflammatory modulation, yet possibly through different pathways. In addition, lactosomes could exert protection by regulating cellular function at the level of the infant gut. Furthermore, these two particles differ in their nutritive roles such that MFGs are a main source of energy for the infant (i.e., Tg-rich cream particles), while lactosomes potentially offer immunomodulatory functionality independent of macronutrient supply. Future mechanistic studies are required to determine what physiological and pathological conditions dictate the function of lactosomes throughout lactation.

Supporting Information Available: Experimental details; tables of proteomes of the MFG and lactosome fractions for samples 1000d08, 1005d08, and 1008d08; and figures of a tandem mass spectrometry spectrum, ESI FT-ICR MS spectra, and a negative mode spectrum. This material is available free of charge via the Internet at http://pubs.acs.org.

LITERATURE CITED

(1) German, J. B.; Dillard, C. J. Composition, structure and absorption of milk lipids: a source of energy, fat-soluble nutrients and bioactive molecules. *Crit. Rev. Food Sci. Nutr.* **2006**, *46*, 57−92.
(2) Mather, I. H.; Keenan, T. W. Origin and secretion of milk lipids. *J. Mammary Gland Biol. Neoplasia* **1998**, *3*, 259−273.

(3) Wooding, F. B. The mechanism of secretion of the milk fat globule. *J. Cell Sci.* **1971**, *9*, 805−821.
(4) Mather, I. H.; Weber, K.; Keenan, T. W. Membranes of mammary gland. XII. Loosely associated proteins and compositional heterogeneity of bovine milk fat globule membrane. *J. Dairy Sci.* **1977**, *60*, 394−402.
(5) Cavaletto, M.; Giuffrida, M. G.; Conti, A. Milk fat globule membrane components—A proteomic approach. *Adv. Exp. Med. Biol.* **2008**, *606*, 129−141.
(6) Sanchez-Juanes, F.; Alonso, J. M.; Zancada, L.; Hueso, P. Glycosphingolipids from bovine milk and milk fat globule membranes: A comparative study. Adhesion to enterotoxigenic Escherichia coli strains. *Biol. Chem.* **2009**, *390*, 31−40.
(7) Michalski, M. C.; Cariou, R.; Michel, F.; Garnier, C. Native vs. damaged milk fat globules: Membrane properties affect the viscoelasticity of milk gels. *J. Dairy Sci.* **2002**, *85*, 2451−2461.
(8) Scow, R. O.; Blanchette-Mackie, E. J.; Smith, L. C. Transport of lipid across capillary endothelium. *Fed. Proc.* **1980**, *39*, 2610−2617.
(9) Michalski, M. C.; Briard, V.; Michel, F.; Tasson, F.; Poulain, P. Size distribution of fat globules in human colostrum, breast milk, and infant formula. *J. Dairy Sci.* **2005**, *88*, 1927−1940.
(10) Couvreur, S.; Hurtaud, C.; Lopez, C.; Delaby, L.; Peyraud, J. L. The linear relationship between the proportion of fresh grass in the cow diet, milk fatty acid composition, and butter properties. *J. Dairy Sci.* **2006**, *89*, 1956−1969.
(11) Lopez, C.; Briard-Bion, V.; Menard, O.; Rousseau, F.; Pradel, P.; Besle, J. M. Phospholipid, sphingolipid, and fatty acid compositions of the milk fat globule membrane are modified by diet. *J. Agric. Food Chem.* **2008**, *56*, 5226−5236.
(12) Argov, N.; Wachsmann-Hogiu, S.; Freeman, S. L.; Huser, T.; Lebrilla, C. B.; German, J. B. Size-dependent lipid content in human milk fat globules. *J. Agric. Food Chem.* **2008**, *56*, 7446−7450.
(13) Wyne, K. L.; Woollett, L. A. Transport of maternal LDL and HDL to the fetal membranes and placenta of the Golden Syrian hamster is mediated by receptor-dependent and receptor-independent processes. *J. Lipid Res.* **1998**, *39*, 518−530.
(14) Hayat, M. *Introduction to Biological Scanning Electron Microscopy*; University Park Press: Baltimore, MD, 1978.
(15) Hayat, M. *Principles and Techniques of Electron Microscopy: Biological Applications*; Cambridge University Press: Cambridge, United Kingdom, 2000.
(16) Argov, N.; Wachsmann-Hogiu, S.; Freeman, S. L.; Huser, T.; Lebrilla, C. B.; German, J. B. Size-Dependent Lipid Content in Human Milk Fat Globules. *J. Agric. Food Chem.* **2008**, *56*, 7446−7450.
(17) Matsuzaki, K.; Murase, O.; Sugishita, K.; Yoneyama, S.; Akada, K.; Ueha, M.; Nakamura, A.; Kobayashi, S. Optical characterization of liposomes by right angle light scattering and turbidity measurement. *Biochim. Biophys. Acta* **2000**, *1467*, 219−26.
(18) Wessel, D.; Flugge, U. I. A Method for the Quantitative Recovery of Protein in Dilute-Solution in the Presence of Detergents and Lipids. *Anal. Biochem.* **1984**, *138*, 141−143.
(19) Pollard, K. S.; Dudoit, S.; van der Laan, M. J. Multiple Testing Procedures: R multtest Package and Applications to Genomics Using R and Bioconductor. *Bioinf. Comput. Biol.* **2005**, 251−272.
(20) Davenport, L.; Dale, R.; Bisby, R.; Cundall, R. Transverse location of the fluorescent probe 1, 6-diphenyl-1, 3, 5-hexatriene in model lipid bilayer membrane systems by resonance excitation energy transfer. *Biochemistry* **1985**, *24*, 4097−4108.
(21) Vinchurkar, M. S.; Bricarello, D. A.; Lagerstedt, J. O.; Buban, J. P.; Stahlberg, H.; Oda, M. N.; Voss, J. C.; Parikh, A. N. Bridging across length scales: multi-scale ordering of supported lipid bilayers via lipoprotein self-assembly and surface patterning. *J. Am. Chem. Soc.* **2008**, *130*, 11164−9.
(22) Folch, J.; Lees, M.; Sloane Stanley, G. H. A simple method for the isolation and purification of total lipides from animal tissues. *J. Biol. Chem.* **1957**, *226*, 497−509.
(23) Smith, D.; Prieto, P. Special considerations for glycolipids and their purification. In *Current Protocols in Molecular Biology*; Ausubel, F. M., et al., Eds.; Wiley: New York, 2001.
(24) Sorensen, L. A liquid chromatography/tandem mass spectrometric approach for the determination of gangliosides GD3 and GM3 in bovine milk and infant formulae. *Rapid Commun. Mass Spectrom.* **2006**, *20*, 3625−3633.
(25) Jensen, R. The lipids in human milk. *Prog. Lipid Res.* **1996**, *35*, 53−92.
(26) Jensen, R. G.; Thompson, M. P. *Handbook of Milk Composition*; Academic Press: San Diego, 1995.
(27) Han, X.; Gross, R. W. Shotgun lipidomics: electrospray ionization mass spectrometric analysis and quantitation of cellular lipidomes directly from crude extracts of biological samples. *Mass Spectrom. Rev.* **2005**, *24*, 367−412.
(28) Jensen, R. G. Lipids in human milk. *Lipids* **1999**, *34*, 1243−1271.
(29) Iwamori, M.; Takamizawa, K.; Momoeda, M.; Iwamori, Y.; Taketani, Y. Gangliosides in human, cow and goat milk, and their abilities as to neutralization of cholera toxin and botulinum type A neurotoxin. *Glycoconjugate J.* **2008**, *25*, 675−683.
(30) Desai, P.; Walsh, M.; Weimer, B. Solid-Phase Capture of Pathogenic Bacteria by Using Gangliosides and Detection with Real-Time PCR? *Appl. Environ. Microbiol.* **2008**, *74*, 2254−2258.
(31) Newburg, D.; Ruiz-Palacios, G.; Morrow, A. Human milk glycans protect infants against enteric pathogens. *Annu. Rev. Nutr.* **2005**, *25*, 37−58.
(32) Kaess, B.; Fischer, M.; Baessler, A.; Stark, K.; Huber, F.; Kremer, W.; Kalbitzer, H.; Schunkert, H.; Riegger, G.; Hengstenberg, C. The lipoprotein subfraction profile: heritability and identification of quantitative trait loci. *J. Lipid Res.* **2008**, *49*, 715.
(33) Admyre, C.; Johansson, S.; Qazi, K.; Filen, J.; Lahesmaa, R.; Norman, M.; Neve, E.; Scheynius, A.; Gabrielsson, S. Exosomes with immune modulatory features are present in human breast milk. *J. Immunol.* **2007**, *179*, 1969.
(34) Mather, I. H.; Jack, L. J. A review of the molecular and cellular biology of butyrophilin, the major protein of bovine milk fat globule membrane. *J. Dairy Sci.* **1993**, *76*, 3832−3850.
(35) Palmer, D. J.; Kelly, V. C.; Smit, A. M.; Kuy, S.; Knight, C. G.; Cooper, G. J. Human colostrum: Identification of minor proteins in the aqueous phase by proteomics. *Proteomics* **2006**, *6*, 2208−2216.
(36) Alain, K.; Karrow, N.; Thibault, C.; St-Pierre, J.; Lessard, M.; Bissonnette, N. Osteopontin: An early innate immune makers of *Escherichia coli* mastitis harbors genetic polymorphisms with possible links with resistance to mastitis. *BMC Genomics* **2009**, *10*, 444.
(37) Ashkar, S.; Weber, G.; Panoutsakopoulou, V.; Sanchirico, M.; Jansson, M.; Zawaideh, S.; Rittling, S.; Denhardt, D.; Glimcher, M.; Cantor, H. Eta-1 (osteopontin): An early component of type-1 (cell-mediated) immunity. *Science* **2000**, *287*, 860.
(38) Chabas, D.; Baranzini, S.; Mitchell, D.; Bernard, C.; Rittling, S.; Denhardt, D.; Sobel, R.; Lock, C.; Karpuj, M.; Pedotti, R. The influence of the proinflammatory cytokine, osteopontin, on autoimmune demyelinating disease. *Science* **2001**, *294*, 1731.
(39) Weber, G.; Ashkar, S.; Glimcher, M.; Cantor, H. Receptor-ligand interaction between CD44 and osteopontin (Eta-1). *Science* **1996**, *271*, 509.
(40) Takahashi, S.; Oki, J.; Miyamoto, A.; Moriyama, T.; Asano, A.; Inyaku, F.; Okuno, A. Beta-2-microglobulin and ferritin in cerebrospinal fluid for evaluation of patients with meningitis of different etiologies. *Brain Dev.* **1999**, *21*, 192−199.
(41) Pettersson-Kastberg, J.; Mossberg, A.; Trulsson, M.; Joong, Y.; Min, S.; Lim, Y.; , J.; Svanborg, C.; Mok, K. alpha-Lactalbumin, engineered to be non-native and inactive, kills tumor cells when in complex with oleic acid: A new biological function resulting from partial unfolding. *J. Mol. Biol.* **2009**, *394*, 994−1010.
(42) Svensson, M.; Håkansson, A.; Mossberg, A.-K.; Linse, S.; Svanborg, C. Conversion of α-lactalbumin to a protein inducing apoptosis. *Proc. Natl. Acad. Sci. U.S.A.* **2000**, *97*, 4221−4226.
(43) Chaby, R. Lipopolysaccharide-binding molecules: Transporters, blockers and sensors. *Cell. Mol. Life Sci.* **2004**, *61*, 1697−1713.
(44) Harris, H.; Grunfeld, C.; Feingold, K.; Rapp, J. Human very low density lipoproteins and chylomicrons can protect against endotoxin-induced death in mice. *J. Clin. Invest.* **1990**, *86*, 696.
(45) Desai, P.; Walsh, M.; Weimer, B. Solid phase capture of pathogenic bacteria using gangliosides and detection with real time PCR. *Appl. Environ. Microbiol.* **2008**, *74*, 2254−2258.

(46) Rueda, R. The role of dietary gangliosides on immunity and the prevention of infection. *Br. J. Nutr.* **2007**, *98*, 68−73.
(47) Shi, J.; Yang, T.; Kataoka, S.; Zhang, Y.; Diaz, A.; Cremer, P. GM Clustering Inhibits Cholera Toxin Binding in Supported Phospholipid Membranes. *Biol. Chem.* **1997**, *272*, 5533−5538.

Received for review June 30, 2010. Revised manuscript received September 15, 2010. Accepted September 20, 2010. This research was supported in part by the National Institute of Environmental Health Sciences (NIEHS) Grant R37 ES02710, the NIEHS Superfund Basic Research Program P42 ES04699, the University of California Davis Center for Children's Environmental Health, NIEHS Grant P01 ES11269, the University of California Discovery Program, California Dairy Research Foundation 09 GEB-01-NH, and U.S. Department of Energy, Office of Basic Energy Sciences through a grant (DE-FG02-04ER46173) from the Biomolecular Materials Program. The funders had no role in study design, data collection and analysis, decision to publish, or preparation of the manuscript.